Heliyon 10 (2024) e29259

Contents lists available at ScienceDirect

Heliyon

journal homepage: www.cell.com/heliyon

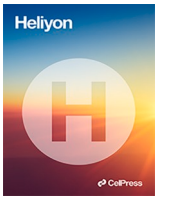

Research article

Electric partial discharges in biodegradable oil-based ferrofluids: A study on effects of magnetic field and nanoparticle concentration

Juraj Kurimský [a], Michal Rajňák [a,b,*], Katarína Paulovičová [b], Miloš Šárpataky [a]

[a] Faculty of Electrical Engineering and Informatics, Technical University of Košice, Letná 9, 04200, Košice, Slovakia
[b] Institute of Experimental Physics SAS, Watsonova 47, 04001, Košice, Slovakia

ARTICLE INFO

Keywords:
Ferrofluids
Magnetic nanoparticles
Transformer oil
Magnetic field
Electrical discharge

ABSTRACT

This paper presents an experimental study of partial discharge activity in ferrofluids based on biodegradable transformer oil and iron oxide nanoparticles. Three ferrofluid samples with low, medium and high nanoparticle concentrations are employed in the research. The basic ferrofluid characterization is followed by a partial discharge experiment exposing the ferrofluids to a high voltage in a needle-plate electrode configuration. The analysis confirms that the apparent charge and number of discharges decrease with increasing nanoparticle concentration. These findings are interpreted with reference to the well-recognised electro-hydrodynamic streamer model. The charge trapping by nanoparticles hinders the ionization and discharge development. The study also focuses on the partial discharge activity in the ferrofluids under the action of a static magnetic field acting perpendicularly to the electric field. A decreasing trend in the number of discharges due to the magnetic field is revealed. A qualitative explanation is provided based on the field-induced cluster formation and charge mobility reduction. The presented experiment and the discussed findings may be valuable for practical application of the ferrofluid in high voltage equipment with a special need for partial discharge suppression.

1. Introduction

The advancement of high-voltage technology necessitates enhancing insulation capabilities and heat transfer efficiency in line with sustainable development, particularly through the utilization of eco-friendly materials [1]. Biodegradable insulating liquids emerge as a viable substitute for mineral oils in liquid insulation applications for high-voltage equipment [2]. The recent approach to enhancing the dielectric properties of biodegradable oils relies on nanoparticles incorporation, so creating stable colloidal suspensions (nanofluids) [3]. Numerous studies have been carried out on the use of appropriately sized nanoparticles and concentrations with the aim to improve the dielectric performance [4–9]. The knowledge on the effect of nanoparticles on dielectric properties of insulating liquids is of importance due to the fact that various nanoparticles (metal and non-metal) can detach from the equipment and leak into the oil [10]. Besides the various physical and chemical properties that determine the suitability of nanofluids for high-voltage applications, the resistance to the partial discharges (PD) is of particular interest, because PD can lead to severe insulation damage and cause unwanted contamination due to chemical processes and mechanical deterioration. In practise it is known that PD occurring in

* Corresponding author. Institute of Experimental Physics SAS, Watsonova 47, 04001, Košice, Slovakia.
E-mail address: rajnak@saske.sk (M. Rajňák).

https://doi.org/10.1016/j.heliyon.2024.e29259
Received 21 December 2023; Received in revised form 18 March 2024; Accepted 3 April 2024
Available online 5 April 2024

insulation not only highlights a local degradation region of the insulation, but also accelerates insulation degradation due to ion bombardment [11]. Thus, investigation of PD aids in determining insulation quality and serves as a diagnostic tool for oils in high-voltage transformers.

Recently, Khelifa et al. [12] conducted a study on synthetic ester (SE) MIDEL 7131 samples mixed with fullerene nanoparticles sized between 4 and 8 nm. The nanoparticle concentrations ranged from 0.1 g/L to 0.5 g/L in steps of 0.1 g/L. Partial discharge parameters were evaluated on the sample that yielded the best results from the AC breakdown voltage measurement, specifically the sample with a concentration of 0.4 g/L. The study revealed a 5.1% improvement in the inception voltage value, but the extinction voltage of partial discharges decreased by 14.98%. Additionally, quantities such as average electric charge, maximum charge, and frequency of discharges showed improvements of 18.18%, 34.63%, and 42%, respectively. The positive effect of nanoparticles on PD activity was described also in Ref. [13] where enhancement of PD inception voltage in natural ester (NE) due to the addition of Al_2O_3 nanoparticles reached values up to 39.3 %. In another study by Sun et al. [14], the PD inception voltage was enhanced by 13.4 % before and 23.8 % after accelerated ageing in mineral oil with TiO_2 nanoparticles. Indeed, the enhancements of PD activity in insulating oils have been reported for various nanoparticles, e.g., $CaCu_3Ti_4O_{12}$ nanoparticles [15] also enhance PD inception voltage up to 34.95 % when dispersed in synthetic ester. Silica and fullerene could also improve PD inception voltage of mineral oil [16]. Besides that, it was demonstrated that an insulating paper impregnated with a SiC nanofluid also exhibits greater resistance to the appearance of partial discharge activity [17].

In the research on nanofluids for electrical engineering applications, a special attention has been paid to magnetic fluids (ferrofluids) [18]. They are colloidal suspensions of magnetic nanoparticles in a liquid carrier exhibiting magnetically driven variations of physical properties due to the interacting magnetic nanoparticles with a magnetic field [19]. As a result, the phenomena like thermomagnetic convection [20] or magneto-dielectric anisotropy [21] may be observed in ferrofluids. In our earlier study we have demonstrated that ferrofluids based on mineral oil and iron oxide nanoparticles are more resistant to PD than pure mineral oil [6]. It

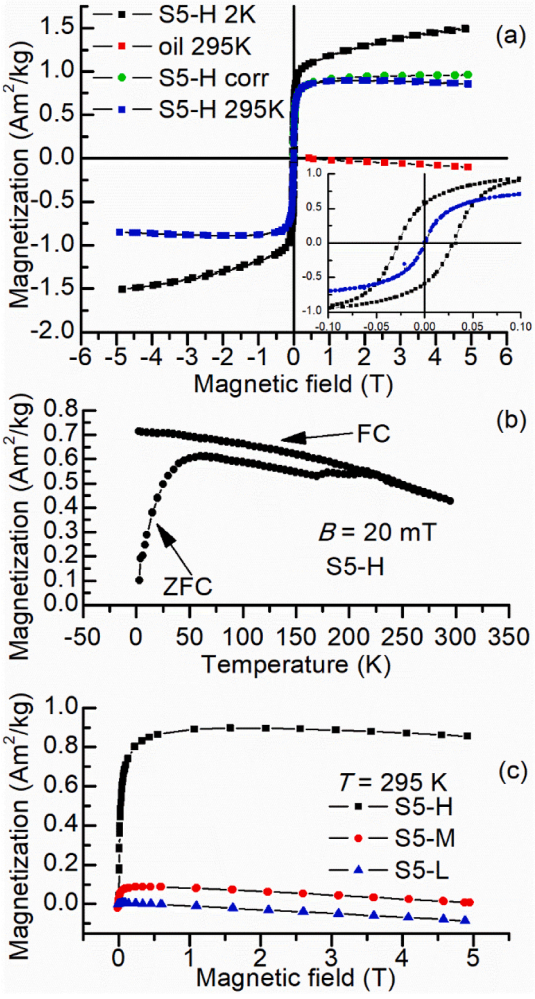

Fig. 1. Isothermal magnetization curves measured on S5–H ferrofluid (a) and temperature-dependent magnetization measured in ZFC and FC regime (b). The bottom graph (c) presents the isothermal magnetizations of all ferrofluid samples measured in the first quadrant.

was found that PD inception voltage increases and the pulse repetition rate decreases with increasing nanoparticle concentration. However, there are less studies focused on the PD activity in ferrofluids in an external magnetic field. On the other hand, the presence of a magnetic field along with the electric field may affect the PD characteristics as per the classical electromagnetic theory. The influence of a magnetic field on PD activity was confirmed even for oils with non-magnetic nanoparticles. For instance, the application of magnetic field on a synthetic ester oil with zeolite particles or copper particles has a remarkable effect on PD activity [22,23]. The effect is associated with the Lorentz force acting on the charged particle moving in the electric field.

The present work examines the behaviour of partial discharges in a ferrofluid based on biodegradable oil (gas-to-liquid technology) and iron oxide nanoparticles of three different concentrations. During the experiment, PD parameters were analyzed and compared under two conditions: with and without the application of a magnetic field. The magnetic field was generated using a pair of permanent magnets. This allowed for an assessment of how the presence of a magnetic field influences the observed PD behaviour.

2. Materials and methods

The ferrofluid samples studied herein are based on a high-performance biodegradable transformer oil Shell Diala S5 BD. The density of the oil at 20 °C is 816 kg/m^3 and kinematic viscosity at 40 °C is 7.4 mm^2/s, as stated by the producer (Shell). In order to prepare the ferrofluids, we have synthesized iron-oxide magnetic nanoparticles by the well-established chemical co-precipitation method [24]. The nanoparticles were precipitated from ferrous and ferric salts in molar rate 1:2 in alkali medium at the temperature of 353 K. In the following step, the nanoparticles were sterically stabilized and coated with a single layer of oleic acid at the temperature range 353–355 K. The coated nanoparticles with hydrophobic character were dispersed in the transformer oil [25]. Then, the obtained ferrofluid sample was diluted with the base oil (herein labelled as S5-0), and three ferrofluid samples with low (S5-L), medium (S5-M) and high (S5–H) nanoparticle concentration have been prepared.

A vibrating sample magnetometer (Cryogenic Limited, UK) was employed to explore magnetic properties of the ferrofluids. The volume of 30 μl of the samples was sealed in a plastic tube and exposed to the magnetization measurements in the static magnetic field ranging from −5 T to 5 T and temperatures from 2 K to 295 K. The isothermal magnetization curves measured on S5–H sample at 2 K and 295 K and the transformer oil are presented in Fig. 1(a). One can see that the magnetization of oil is purely of diamagnetic nature. When subtracting this diamagnetic contribution from the total ferrofluid magnetization one obtains the corrected magnetization with a slightly higher saturation. The magnetization curve resulting from this correction is labelled as S5–H corr. The magnetization of saturation of S5–H at room temperature is found to be 0.898 Am^2/kg, while the corrected magnetization of saturation is 0.958 Am^2/kg. This saturation magnetization naturally increases as the thermal energy decreases. From the inset of Fig. 1(a) one can further see that the room temperature magnetization curve exhibits zero hysteresis and remanence and suggests the superparamagnetic nature of the nanoparticles. On the other hand, the magnetic moments of the nanoparticles are found blocked at 2 K as seen from the remarkable hysteresis in the magnetization curve at this temperature. The transition from the blocked to superparamagnetic state occurs around 50 K. This is concluded from the zero-field-cooled (ZFC) magnetization curve shown in Fig. 1(b). The significant shoulder around 50 K reveals the area of blocking temperatures. The further bifurcation of the ZFC and field-cooled (FC) curves starting at 215 K reflects the solidification of the transformer oil. In Fig. 1(c) we provide the comparison of the magnetization curves in the first quadrant of the three ferrofluid samples.

One can observe the remarkable effect of the nanoparticle concentration. The saturation magnetization of S5-M can be determined at the field of 0.34 T, yielding the value 0.087 Am^2/kg, while for S5-L the value of 0.0046 Am^2/kg is determined at 0.072 T. At higher magnetic fields, the magnetizations of these ferrofluids conspicuously decrease as a result of the diamagnetic contribution of the transformer oil to the ferrofluid magnetization. The ferrofluids' saturation magnetization M_{SF} values were used to determine a magnetic mass fraction φ in the ferrofluids according to the relation $\varphi = (M_{SF}/M_{SP}) \times 100$, where M_{SP} is the magnetization of saturation of the dry powder nanoparticles with the experimentally found value of 73 Am^2/kg. The determined magnetic mass fraction of S5–H, S5-M and S5-L is 1.2%, 0.1% and 0.006%, respectively. The magnetization data of S5–H in the first quadrant have been further analyzed in order to reveal the nanoparticle size distribution. The analysis is based on the application of the superposition Langevin fit function [26]. The obtained particle size distribution is shown in Fig. 2.

The dynamic magnetic response of the ferrofluids was tested by means of a susceptometer (Imego, Dynomag, SE). The complex

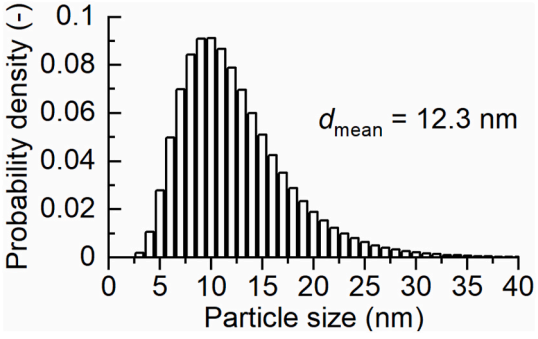

Fig. 2. Magnetic nanoparticle size distribution obtained from the magnetization measurement.

magnetic susceptibility was measured on 200 μl of ferrofluid samples in alternating current (AC) magnetic field with frequencies ranging from 1 Hz to 250 kHz. The amplitude of the excitation field is 0.5 mT. The obtained spectra of real and imaginary component of the complex susceptibility are presented in Fig. 3(a and b). As the figure shows, the real and imaginary susceptibility of each ferrofluid exhibits quasi constant behavior in the applied frequency range. This fact is associated with the small nanoparticle size and relatively narrow size distribution. The high-concentrated ferrofluid S5–H shows a tendency to decreases the susceptibility at the upper frequency limit. This can be due to the possible aggregates in this ferrofluid and their magnetic relaxations reflected in the emerging relaxation maximum in the imaginary susceptibility near the high frequency limit. The average real susceptibility magnitude of the ferrofluids is 3×10^{-2}, 3×10^{-3} and 3×10^{-4} for S5–H, S5-M and S5-L, respectively.

To characterize the studied samples from electrical conductivity point of view, we have employed the Eltel Model ADTR-2K Plus test set equipment. The direct current electrical conductivity was measured at temperature of 295 K. The liquids were poured into a specialized cylindrical stainless-steel cell (2 mm gap between the concentric cylinders, 100 mm high) powered by a direct voltage of 1 kV. The obtained values of electrical conductivity of oil, S5-L, S5-M, S5–H samples are 0.004539 pS/cm, 0.3028 pS/cm, 2.699 pS/cm, and 52.36 pS/cm, respectively.

The measurement of partial discharges was examined according to the IEC 60270 standard, as well as the specialized standard for measuring partial discharges in insulating oils, namely the IEC 61294 [27]. Note that according to the IEC 61294 standard, discharges with an apparent charge exceeding 100 pC should be included in the statistical analysis. However, due to the sensitivity settings, and the low frequency of discharges observed in the most resilient samples, all discharges with an apparent charge above 3 pC were considered in this particular measurement. Interference that could potentially impact the measurement results was limited to around the 2 pC threshold, as depicted in Fig. 4. This figure also displays the applied voltage profile, which reached a maximum level of 20 kV at a frequency of 50 Hz, with a rate of rise 1 kV/s. The voltage ramp was achieved using a APS-7050E linear AC power supply (GWINSTEK, Good Will Instrument Co., TW). The duration of voltage application to the electrode system was 5 min for reaching the desired voltage amplitude and 40 s for both the voltage rise and fall to the desired values.

The partial discharge charge, generated by the corona and streamers, was induced by applying a voltage to a needle electrode and a ground plate configuration. The needle electrode was immersed in the test liquid contained in a 30 ml container (Silanized Glass Vial, Thermo Scientific, CA). The distance between the needle electrode and the plate was maintained at 20 ± 0.05 mm. Tungsten Carbide Needle (Fine Science Tools, DE) was used. The diameter of tip-curvature is around 2 μm, as revealed by an optical microscope (Fig. 5). Partial discharges were measured using an MPD600 PD measurement system and the mtronix v1.0 software (Omicron Electronics, AT). The setup calibration of the induced charge was conducted using a Tettex PD calibrator type 9216 device (Tettex Instruments, CH). Thus, the measurement uncertainty of PD level in our experiment is ±2 % of calibrated PD value, the uncertainty of voltage is ±0.05 % of calibrated voltage and the frequency is measured with uncertainty of ±1 ppm, as stated by the manufacturer. To prevent degradation of the measured sample or damage of the needle electrode (change in the tip curvature), a h.v. 100 kOhm resistor was added in series behind the voltage transformer to reduce the magnitude of the currents. The impact of the curvature radius on partial discharge parameters has been discussed in Ref. [27]. The measurements of partial discharges were carried out at ambient conditions.

As structural and physical properties of ferrofluids are controllable by magnetic fields (e.g. effect on electroconvection [28] and magnetic nanoparticle assembly at ferrofluid/solid interface [29]), we also performed the measurements of the partial discharges under an influence of an external static magnetic field. This magnetic field was generated by attaching two permanent magnets (NdFeB) to the container wall, as illustrated in Fig. 6. Thus, the vector of the magnetic field induction between the magnets is perpendicular to the electric field intensity between the electrodes. The magnitude of the magnetic field induction at the location of the tip electrode reached a value of 60 mT. The value was found experimentally by the Gaussmeter HGM09S (MAGSYS Magnet Systeme, DE).

3. Results

When analysing the partial discharge parameters, the results are categorized into two main groups: discharges occurring during the positive half-period and discharges occurring during the negative half-period of the applied alternating voltage with a frequency of 50 Hz. In these measurements, discharges in the positive half-cycle with an apparent charge exceeding 50 pC are associated with streamers. The streamers are propagating ionization fronts with self-organized field enhancement at their tips [30]. Their apparent

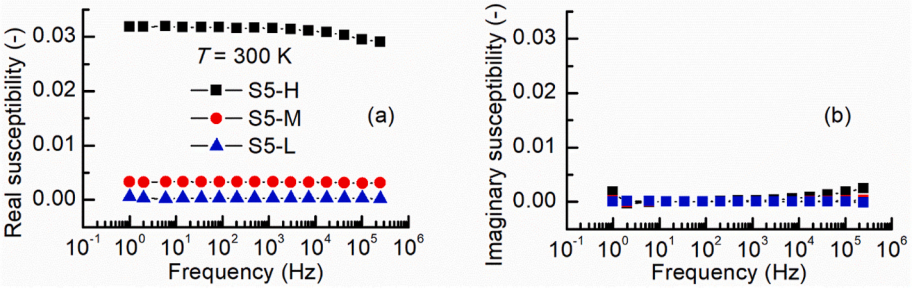

Fig. 3. Real (a) and imaginary (b) part of magnetic AC susceptibility of the ferrofluids versus the frequency of the magnetic field.

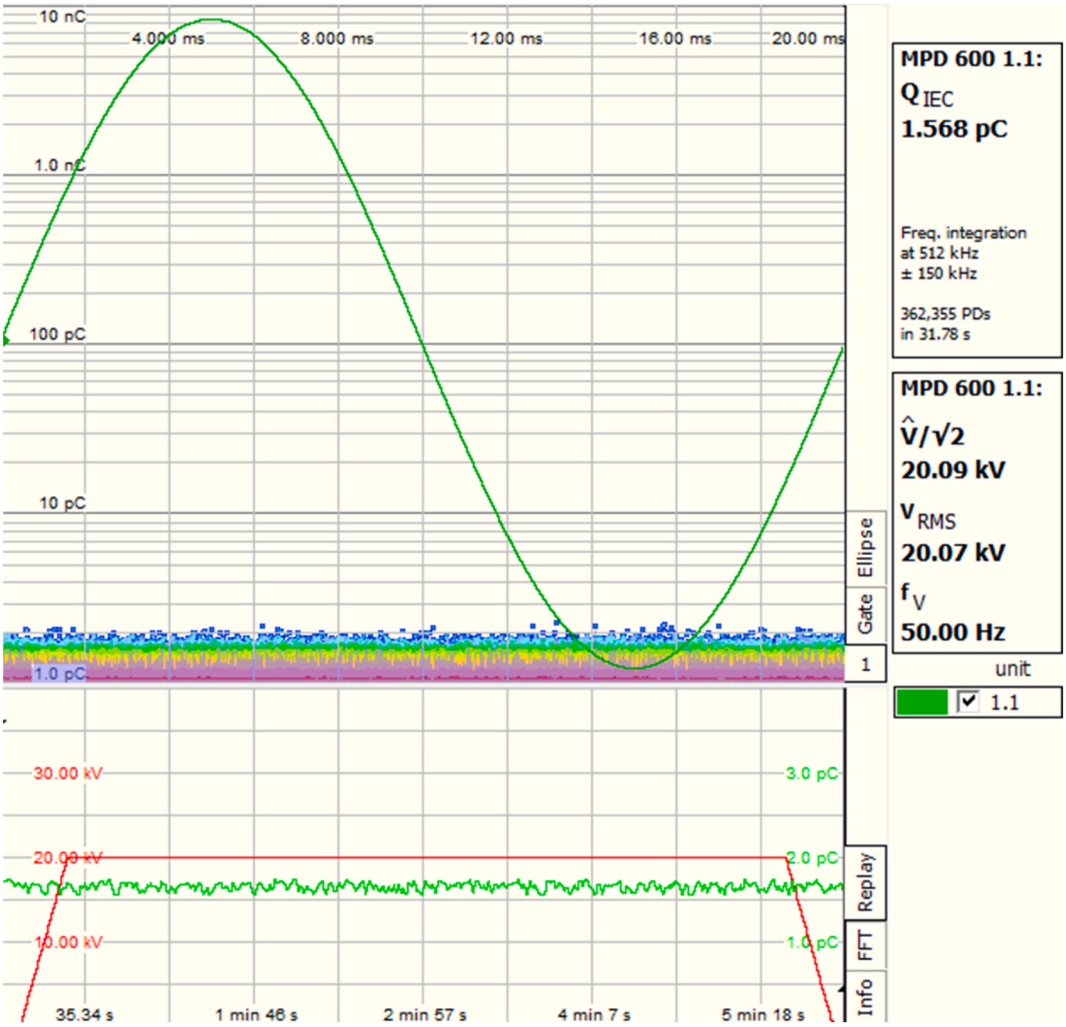

Fig. 4. Value, course of disturbance during measurement of partial discharges and behaviour of the voltage ramp.

charge value is higher compared to the values observed in the negative half-cycle, where corona discharges are observed near the tip of the electrode. These findings were previously published in the work by Kurimský et al. [6]. Owing to the experimental setup, the inception nor extinction voltage of the partial discharges were not determined. This is because the partial discharges gradually occurred over a 5-min period at the constant voltage level, rather than during the rising or decreasing voltage. Note that the inception and extinction voltage should be measured during the voltage rise and drop, respectively [27].

To determine the quality of the samples, it is necessary to consider both the magnitude of the apparent charge (Fig. 7) and the number of the measured discharges (Fig. 8). Clearly, a higher quality of insulation is indicated by lower values of the apparent charge and a reduced number of discharges. This is because partial discharges in insulating liquids contribute to the gradual degradation of the samples. Therefore, a decrease in the apparent charge and number of discharges signifies an improvement in the insulation quality.

Fig. 7 clearly demonstrates that the magnitude of the apparent charge decreases as the nanoparticle concentration increases. In the negative half-period, the value of the apparent charge remains relatively unchanged. However, it should be noted that at the highest concentration of nanoparticles S5–H, no discharges occurred during the negative half-period. In the case of low (S5-L) and medium (S5-M) concentrations of magnetite nanoparticles in the base oil, the apparent charge at the positive half cycle decreased by more than threefold as compared with the pure oil S5-0. The positive apparent charge in S5-L is of about 20% greater than that in S5-M sample. At the highest nanoparticle concentration (S5–H), the average apparent charge decreased to 18.2 pC constituting 96% decrease in comparison with the apparent charge detected in the pure oil S5-0. The reason of the more significant effect of the nanoparticles on the change in the apparent charge (pC) during the positive half-period is associated with the nature of the discharges. As mentioned above, the discharges in the positive half-cycle with an apparent charge exceeding 50 pC are represented by streamers. The streamers reach a significantly greater volume of the liquid than the local corona discharges appearing just near the electrode tip. Thus, a significantly greater number of nanoparticles are involved in the interaction with the streamers at the positive half period, leading to the more remarkable suppression of the apparent charge.

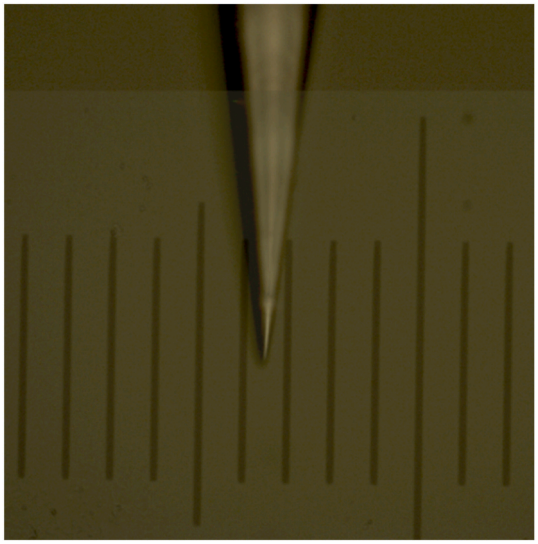

Fig. 5. The microscopic photography showing the radius of the needle electrode tip curvature with a scale of 10 μm per division.

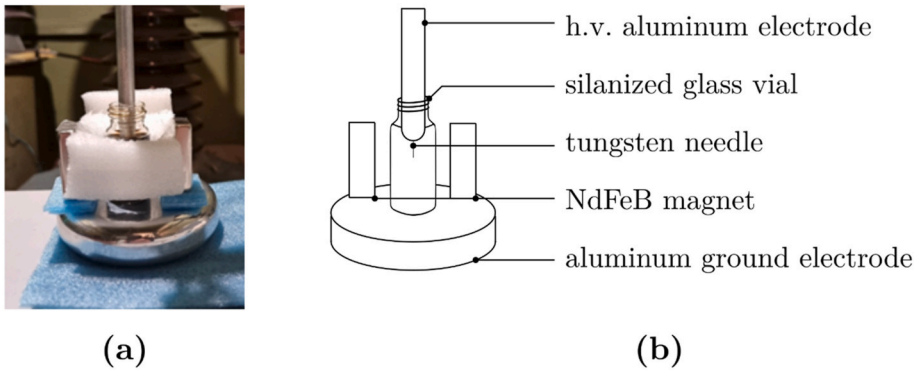

Fig. 6. The experimental setup with the electrode system for measuring partial discharges with the attached pair of permanent magnets. (a) real setup, (b) explanatory sketch (not to scale).

In contrast to the apparent charge values, the number of discharges does not exhibit an improvement in the quality of the insulating oil with the low and medium concentrations of nanoparticles (Fig. 8). On the other hand, the number of discharges during both the positive and negative half-periods follows a similar pattern, displaying a decreasing trend with increasing nanoparticle concentration. Specifically, at low and medium concentrations of Fe_3O_4 nanoparticles, there is a significant increase in the number of discharges during the positive half-period, accompanied by a decrease in the number of discharges during the negative half-period. When considering the cumulative discharges throughout the entire voltage cycle, the lowest concentration results in an increase in the number of discharges. However, at the medium concentration, there is a slight decrease in the total number of partial discharges in the liquid. At the highest concentration of nanoparticles, the number of partial discharges significantly reduces to only six discharges during the measurement.

The influence of the external magnetic field on the values of the apparent charge and the number of discharges is presented in Figs. 9 and 10, respectively.

Fig. 9 illustrates the changes in the apparent charge after the application of an external magnetic field. In the negative half-period of the applied voltage, the value of the apparent charge remains relatively unchanged at the low concentration of nanoparticles. However, at a medium concentration, a significant increase in the apparent charge is observed. Notably, no partial discharges were observed in the negative half-period at the highest concentration of nanoparticles. Regarding the discharge activity in the positive half-period, it is important to note that the average apparent charge increased at all investigated concentrations of magnetite nanoparticles upon application of the magnetic field. The calculated percentage increase is 19.1 %, 1.4 % and 48.9 % for low, medium and high concentrations of nanoparticles, respectively.

Contrary to the apparent charge, Fig. 10 demonstrates a decreasing trend in the number of discharges in nanofluids. The exception is the sample with a medium concentration of nanoparticles where the number of discharges at negative half cycle slightly increased.

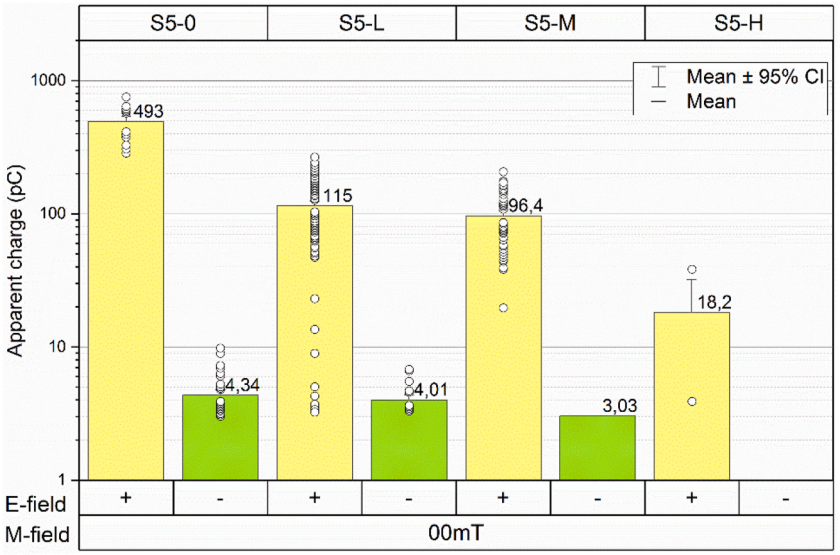

Fig. 7. Apparent charge in the tested samples in the positive (yellow) and negative (green) half-period of the applied voltage. The circle symbols in the bar graph indicate the individual discharges. (For interpretation of the references to colour in this figure legend, the reader is referred to the Web version of this article.)

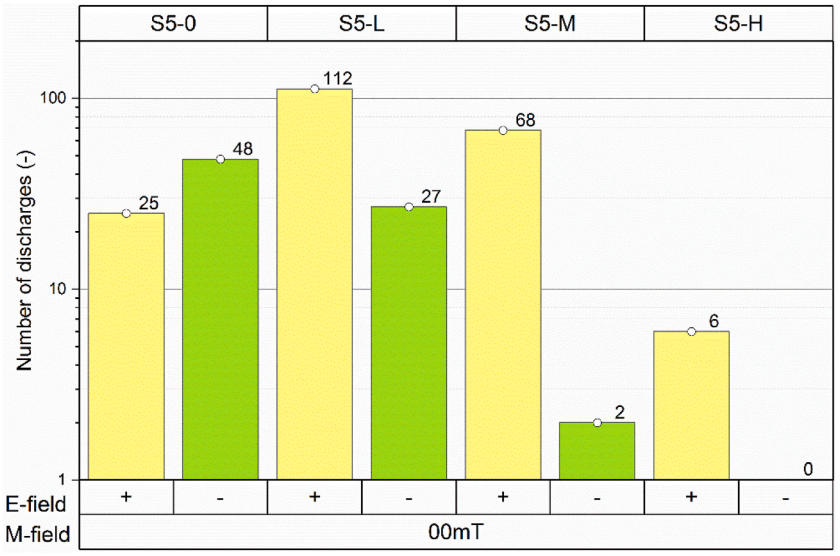

Fig. 8. The number of discharges in the tested samples in the positive (yellow) and negative (green) half-period of the applied voltage. (For interpretation of the references to colour in this figure legend, the reader is referred to the Web version of this article.)

Particularly in the positive half-period of the applied voltage, a significant reduction in the number of discharges is observed, with the percentage difference increasing as the nanoparticle concentration rises. At the highest concentration of nanoparticles, the influence of the external magnetic field causes the number of discharges to decrease considerably, reaching a value of 1, indicating that partial discharges nearly disappear completely. The results of the research findings are summarized in Table 1.

4. Discussion

Within theoretical interpretation of the observed PD activity in transformer oils and nanofluids, one must realize that electron avalanche and space charge distribution are fundamental steps of discharge processes. The space charge distribution refers to the collection of electric charges treated as a continuum of charge distributed over a region of the liquid rather than distinct point-like charges. The electron avalanche constitutes a charge multiplication process. It is driven by the collisional ionization, when electron injected in the liquid under the high electric field strength can ionize the other liquid molecules by collisions. This process takes place

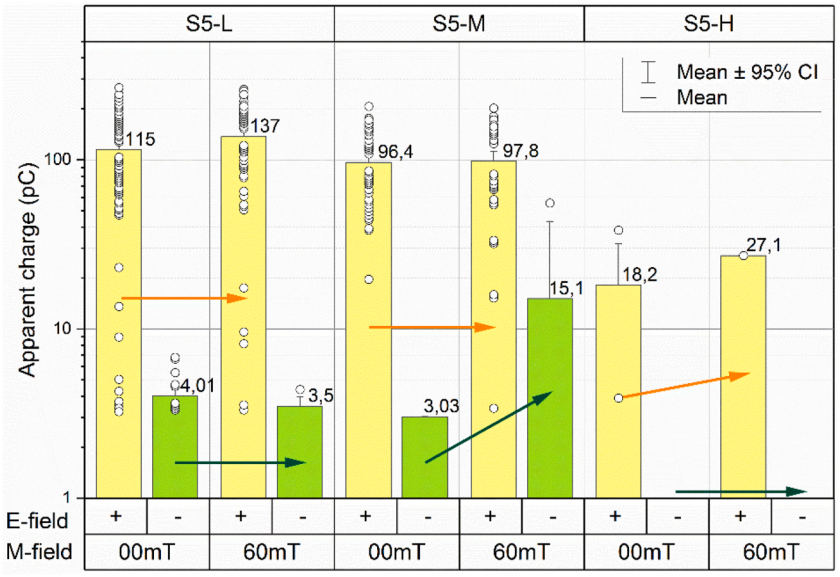

Fig. 9. Apparent charge in the tested samples in the positive (yellow) and negative (green) half-period of the applied voltage. The circle symbols on the bar graphs indicate individual discharges. The arrows show the increase or decrease of the values after the application of an external magnetic field. (For interpretation of the references to colour in this figure legend, the reader is referred to the Web version of this article.)

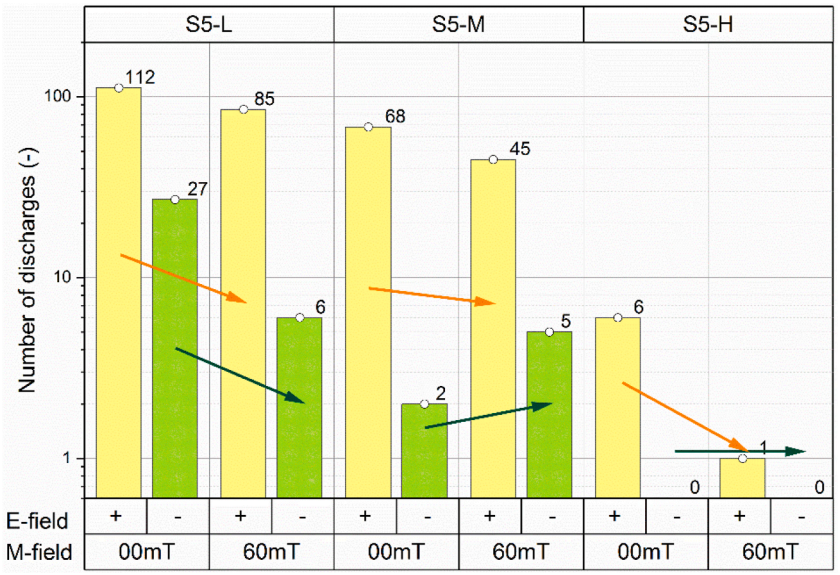

Fig. 10. The number of discharges in the tested samples in the positive (yellow) and negative (green) half-period of the applied voltage. The arrows show the increase or decrease of the values after the application of an external magnetic field. (For interpretation of the references to colour in this figure legend, the reader is referred to the Web version of this article.)

when the energy received by the electron from the electric field between two subsequent collisions is comparable to the ionization energy of the molecules [31]. There are four charge generation mechanisms considered in transformer oil under high electric field, namely weak electrolyte ionization, field emission, impact ionization and field ionization. It has been shown that the field ionization is the main source of electrons and positive ions in transformer oil [32], and it can be expressed as follows

$$G(|\boldsymbol{E}|) = \frac{q^2 n_i a |\boldsymbol{E}|}{h} \exp\left(-\frac{\pi^2 m a \Delta_i^{\,2}}{q h^2 |\boldsymbol{E}|} \right) \tag{1}$$

where q is the elementary charge, n_i is the density of ionizable oil molecules, a is the molecular separation distance, $\boldsymbol{E}$ is the electric field intensity, h is Planck's constant, m is the free electron mass, and Δ_i denotes different ionization potentials. Once the charges are

Table 1
Results of measurement of partial discharges without and with the external magnetic field in Shell Diala S5 BD oil and the nanofluids with magnetite nanoparticles. Applied AC voltage 20 kV rms.

Sample-field	Voltage Period Polarity	Number of PD (−)	Apparent Charge Mean (pC)	Apparent Charge Standard Deviation (pC)	Apparent Charge SD of mean (pC)	Apparent Charge Minimum (pC)	Apparent Charge Median (pC)	Apparent Charge Maximum (pC)
S5-0-0 mT	+	25.00	493.33	115.34	23.07	285.85	497.44	753.69
	–	48.00	4.34	1.46	0.21	3.03	3.81	9.83
S5-L-0mT	+	112.00	114.53	56.04	5.29	3.25	114.86	266.73
	–	27.00	4.01	0.94	0.18	3.32	3.64	6.79
S5-*M*-0mT	+	68.00	96.42	38.49	4.67	19.64	90.13	206.91
	–	2.00	3.03	0.00	0.00	3.03	3.03	3.03
S5–H-0mT	+	6.00	18.18	13.10	5.35	3.90	17.56	38.37
	–	0.00	–	–	–	–	–	–
S5-L-60mT	+	85.00	137.07	58.50	6.35	3.32	139.75	260.64
	–	6.00	3.50	0.44	0.18	3.17	3.32	4.38
S5-*M*-60mT	+	45.00	97.84	47.22	7.04	3.40	94.39	202.19
	–	5.00	15.09	22.63	10.12	3.40	5.91	55.51
S5–H-60mT	+	1.00	27.14	–	–	27.14	27.14	27.14
	–	0.00	–	–	–	–	–	–

generated, the subsequent electron avalanche and space charge distribution depend on the mobility of charge carriers, including electrons and positive and negative ions [33]. It is clear that the charge mobility will be further influenced by the dispersed nanoparticles in the oil. Their influence is well understood when considering the well-recognised electro-hydrodynamic streamer model [34]. Based on this consideration, the added nanoparticles have a trapping effect on the electrons in a streamer with subsequent reduction of its length and the development rate. Let's recall that the charge trapping is provided by the nanoparticles themselves and by the electrical double layer forming around the nanoparticle surface [35]. The electron trapping by nanoparticles will be active until the nanoparticles are charged to saturation. The total amount of the electron charge captured by the polarized nanoparticle is

$$Q_s = -12\pi\varepsilon\varepsilon_0 E R^2 \tag{2}$$

where ε is the relative permittivity of transformer oil, E is the applied electric field intensity and R is the nanoparticle radius. Then, the negative nanocomposite ion density is given as

$$\left|\rho_{npsat}\right| = n_{np}|Q_s| \tag{3}$$

with n_{np} denoting the density of ionizable nanoparticles. The nanoparticles charged in the electric field are then subjected to the resistance action of transformer oil when migrating through the oil. The mobility of the nanocomposite ions under the action of the electric field is

$$\mu_{np} = \frac{Q_s}{6\pi\eta R} \tag{4}$$

where η is the viscosity of transformer oil [34]. It is clear that the mobility of the charge carriers will affect the magnitude of PD and the extinction of the PD.

The above described consideration can explain the PD activity observed in this study without the action of the external magnetic field. Before the occurrence of PD in the ferrofluids, the nanoparticles get polarized and follow the AC electric field changes. The nanoparticles polarization affects the electric field distribution. Then, the generated charges (electrons, ions) follow the electric field lines and charge (get trapped) the nanoparticle surfaces. This mechanism hinders further ionization and discharge development. In our results, that effect is reflected in the decreasing apparent charge (pC) with increasing nanoparticle concentration (Fig. 7). This is true because the more nanoparticles can trap more free charge. On the other hand, at higher nanoparticle concentration there is a higher probability of nanoparticle aggregates formation. The increasing radius of nanoparticle objects due to the aggregation remarkably slows down the mobility of the charged aggregates leading to smaller apparent charge and lower number of discharges. The decreasing trend in the number of discharges with increasing nanoparticle concentration (Fig. 8, especially at negative half-period) may be associated with the limited process of charge generation (electrons, ions) according to equation (1). One can assume that the constant volume of ferrofluids with various nanoparticle concentrations contains various densities of ionizable oil molecules n_i. This parameter decreases with increasing nanoparticle concentration, and therefore the number of charges potentially generated due to the field ionization decreases, too. This is crucial because the generated charges may support further collisional ionization or may form local centres of high electric fields, which may induce local partial discharges, e.g. in nearby bubbles.

Upon application of the external magnetic field on the ferrofluid, the conditions for PD development change markedly. First of all, the magnetic nanoparticles interact with the field and may form chain-like clusters oriented in the field direction [36]. In our experiment it is perpendicular to the electric field direction, as understood from Fig. 6. The susceptible magnetic response of the employed ferrofluid nanoparticles at the acting 60 mT is confirmed in Fig. 1(a). Let's remind that in the absence of the magnetic field the nanoparticle interactions are absent due to their superparamagnetic nature at the room temperature, as confirmed in Fig. 1(a and b). Based on the above discussion one can see that even though the induced clusters can trap the free charge, their mobility is remarkably slower because of the inverse relation to the nanocomposite radius (4). Owing to that mechanism there are less free individual nanoparticles with higher mobility than that of the clusters and therefore the number of discharges tends to decrease in the applied magnetic field, as revealed in Fig. 10. Indeed, the number of discharges decreases with the applied magnetic field but the apparent charge remains practically at the same level or increases. That implies that the less frequent discharges are more intensive. Another crucial physical condition in the PD experiment with the external magnetic field is related to the influence of the magnetic field on the charge carrier movement. It is well-know that this influence results in the action of Lorentz force $\boldsymbol{F}_L$ given as

$$\boldsymbol{F}_L = q \bullet [(\boldsymbol{v} \times \boldsymbol{B})] \tag{5}$$

where q is the nanoparticle's electric charge, $\boldsymbol{v}$ is its velocity and $\boldsymbol{B}$ is the magnetic flux density. This force applies to the movement of both, the free generated charges (electron and ions) and the charged nanoparticles due to the charge trapping. Since the direction of force expressed in (5) is the cross product of velocity and magnetic flux density, the Lorentz force always acts perpendicular to the direction of motion, causing the charges and charged nanoparticles to move in a circular motion. Therefore, the total force that acts on the charged nanoparticles due to both electric and magnetic fields is given by [23]

$$\boldsymbol{F} = q \bullet [\boldsymbol{E} + (\boldsymbol{v} \times \boldsymbol{B})] \tag{6}$$

The induced circular motion of charges and charged nanoparticles is therefore considered as another reason of the decreased charged mobility and the related decrease in the number of discharges.

The found tendency of the magnetic field to supress the partial discharge activity in ferrofluids is positive, especially when

considering the application of ferrofluids in high-voltage electrical equipment. However, such ferrofluids in practise may be exposed to various magnetic field gradients and distributions, where sharp anisotropic nanoparticle clusters may be formed. Under such conditions, the partial discharges can be initiated just at the polarized cluster inhomogeneities. Nevertheless, this is not the case in the quasi homogenous magnetic field, as presented herein.

Finally, let's remark the study's limitations and recommendations for a future study. As partial discharges in insulating liquids contribute to their degradation, it is valuable to consider the role of the degradation products in another partial discharge activity. The gas released from degradation, along with the nanoparticles and the carrier liquid, will jointly form a complex solid-liquid-gas multi-phase dynamic flow and interface behavior. The complex multi-phase flow and interface behavior may form non-uniform electric field. Thus, it may contribute to partial discharge activities and it needs to be considered in the future analysis of the failure mechanism of the transformer oil insulation. Another limitation of that study is associated with the black colour of the ferrofluids. The opacity of the ferrofluids does not allow the precise assessment of the PD activity based on the lightning effects accompanying the PD events. On the other hand, the acoustic inspections of the PD activity in ferrofluids may bring valuable insights in a future study.

5. Conclusion

In summary, three ferrofluid samples with iron oxide nanoparticles have been prepared on biodegradable transformer oil. The ferrofluids exhibit lower partial discharge activity than transformer oil. The conclusion is based on the observed decrease in the apparent charge and number of discharges with increasing nanoparticle concentration. That effect may be explained with the electron trapping model, where the charged nanoparticles migration plays a key role in the development or extinction of the discharges. Moreover, the applied magnetic field tends to decrease the number of discharges. It is concluded that the effect stems from the field induced nanoparticle chain formation and further reduction in the mobility of charged clusters. As the magnetic field acts in perpendicular to the electric field, the Lorentz force contributes to the charge carrier mobility reduction, and can contribute to the reduction of the number of discharges.

Data availability statement

Data will be made available on request.

Funding

This research was funded by the Slovak Academy of Sciences and Ministry of Education in the framework of project VEGA 2/0029/24, 1/0154/21, and Slovak Research and Development Agency under contract No. APVV-18-0160 and APVV-22-0115.

CRediT authorship contribution statement

Juraj Kurimský: Data curation, Conceptualization, Formal analysis, Investigation, Methodology, Software, Supervision, Writing – review & editing. **Michal Rajňák:** Writing – review & editing, Project administration, Methodology, Investigation, Funding acquisition, Data curation, Conceptualization, Writing – original draft. **Katarína Paulovičová:** Validation, Methodology, Investigation, Data curation. **Miloš Šárpataky:** Writing – original draft, Visualization, Investigation, Data curation, Formal analysis.

Declaration of competing interest

The authors declare that they have no known competing financial interests or personal relationships that could have appeared to influence the work reported in this paper.

Acknowledgment

The authors acknowledge the projects implementation: Innovative Testing Procedures for 21st Century Industry ITMS: 313011T565, Operational Programme Integrated Infrastructure (OPII) by the ERDF. The authors would like to acknowledge Professor Zbygniew Rozynek, Faculty of Physics, Adam Mickiewicz University, Poznań, Poland, for his expert advisory in the early stages of the study.

References

[1] M. Rafiq, Y.Z. Lv, Y. Zhou, K.B. Ma, W. Wang, C.R. Li, Q. Wang, Use of vegetable oils as transformer oils – a review, Renew. Sustain. Energy Rev. 52 (2015) 308–324, https://doi.org/10.1016/J.RSER.2015.07.032.

[2] M. Šárpataky, J. Kurimský, M. Rajňák, Dielectric fluids for power transformers with special emphasis on biodegradable nanofluids, Nanomaterials 11 (2021) 2885, https://doi.org/10.3390/NANO11112885, 11 (2021) 2885.

[3] M. Rafiq, Y. Lv, C. Li, A review on properties, opportunities, and challenges of transformer oil-based nanofluids, J. Nanomater. 2016 (2016), https://doi.org/10.1155/2016/8371560.

[4] M.R. Hussain, Q. Khan, A.A. Khan, S.S. Refaat, H. Abu-Rub, Dielectric performance of magneto-nanofluids for advancing oil-immersed power transformer, IEEE Access 8 (2020) 163316–163328, https://doi.org/10.1109/ACCESS.2020.3021003.

[5] M. Šárpataky, J. Kurimský, M. Rajňák, K. Paulovičová, M. Krbal, L. Pelikán, Synthetic and natural ester-based nanofluids with fullerene and magnetite nanoparticles – an experimental AC breakdown voltage study, J. Mol. Liq. 368 (2022) 120802, https://doi.org/10.1016/J.MOLLIQ.2022.120802.

[6] J. Kurimský, M. Rajňák, R. Cimbala, J. Rajnič, M. Timko, P. Kopčanský, Effect of magnetic nanoparticles on partial discharges in transformer oil, J. Magn. Magn Mater. 496 (2020) 165923, https://doi.org/10.1016/J.JMMM.2019.165923.

[7] H. Khelifa, A. Beroual, E. Vagnon, Effect of conducting, semi-conducting and insulating nanoparticles on AC breakdown voltage and partial discharge activity of synthetic ester: a statistical analysis, Nanomaterials 12 (12) (2022) 2105, https://doi.org/10.3390/NANO12122105 (2022) 2105.

[8] A. Beroual, U. Khaled, Statistical investigation of lightning impulse breakdown voltage of natural and synthetic ester oils-based Fe3O4, Al2O3and SiO2Nanofluids, IEEE Access 8 (2020) 112615–112623, https://doi.org/10.1109/ACCESS.2020.3003246.

[9] A. Beroual, H. Duzkaya, AC and lightning impulse breakdown voltages of natural ester based fullerene nanofluids, IEEE Trans. Dielectr. Electr. Insul. 28 (2021) 1996–2003, https://doi.org/10.1109/TDEI.2021.009772.

[10] F. Atalar, A. Ersoy, P. Rozga, Experimental investigation of the effect of nano particles on the breakdown strength of transformer liquids by harmonic current analysis, Elec. Power Syst. Res. 221 (2023) 109390, https://doi.org/10.1016/J.EPSR.2023.109390.

[11] G.C. Montanari, A. Cavallini, Partial discharge diagnostics: from apparatus monitoring to smart grid assessment, IEEE Electr. Insul. Mag. 29 (2013) 8–17, https://doi.org/10.1109/MEI.2013.6507409.

[12] H. Khelifa, E. Vagnon, A. Beroual, AC breakdown voltage and partial discharge activity in synthetic ester-based fullerene and Graphene nanofluids, IEEE Access 10 (2022) 5620–5634, https://doi.org/10.1109/ACCESS.2022.3140928.

[13] N.A. Mohamad, N. Azis, J. Jasni, M.Z.A. Mohd Zainal, R. Yunus, Z. Yaakub, Experimental study on the partial discharge characteristics of palm oil and coconut oil based Al2O3 nanofluids in the presence of sodium Dodecyl Sulfate, Nanomaterials 11 (11) (2021) 786, https://doi.org/10.3390/NANO11030786 (2021) 786.

[14] Z. Sun, Y. Ge, Y. Lv, M. Huang, C. Li, Y. Du, The effects of TiO2 nanoparticles on insulation and charge transport characteristics of aged transformer oil, Proc. - IEEE Int. Conf. Dielectr. Liq. 2019-June (2019), https://doi.org/10.1109/ICDL.2019.8796677.

[15] P. Thomas, N.E. Hudedmani, R.T.A.R. Prasath, N.K. Roy, S.N. Mahato, Synthetic ester oil based high permittivity CaCu3Ti4O12 (CCTO) nanofluids an alternative insulating medium for power transformer, IEEE Trans. Dielectr. Electr. Insul. 26 (2019) 314–321, https://doi.org/10.1109/TDEI.2018.007728.

[16] H. Jin, P. Morshuis, A.R. Mor, J.J. Smit, T. Andritsch, Partial discharge behavior of mineral oil based nanofluids, IEEE Trans. Dielectr. Electr. Insul. 22 (2015) 2747–2753, https://doi.org/10.1109/TDEI.2015.005145.

[17] K.N. Koutras, S.N. Tegopoulos, V.P. Charalampakos, A. Kyritsis, I.F. Gonos, E.C. Pyrgioti, Breakdown performance and partial discharge development in transformer oil-based metal Carbide nanofluids, Nanomaterials 12 (12) (2022) 269, https://doi.org/10.3390/NANO12020269 (2022) 269.

[18] S. Odenbach, Colloidal Magnetic Fluids : Basics, Development and Application of Ferrofluids, Springer Verlag, 2009.

[19] R.E. Rosensweig, Ferrohydrodynamics, Dover Publications, 2013. https://books.google.sk/books/about/Ferrohydrodynamics.html?id=ng_DAgAAQBAJ&redir_esc=y. (Accessed 28 April 2019).

[20] I. Nkurikiyimfura, Y. Wang, Z. Pan, Heat transfer enhancement by magnetic nanofluids—a review, Renew. Sustain. Energy Rev. 21 (2013) 548–561, https://doi.org/10.1016/J.RSER.2012.12.039.

[21] F. Herchl, K. Marton, L. Tomo, P. Kopanský, M. Timko, M. Koneracká, I. Kolcunová, Breakdown and partial discharges in magnetic liquids, J. Phys. Condens. Matter 20 (2008) 204110, https://doi.org/10.1088/0953-8984/20/20/204110.

[22] N. Guvvala Mridula, R. Sarathi, R. Vinu, Effect of zeolite addition on partial discharge and dielectric behavior of thermally aged synthetic ester fluid under external magnetic field, IEEE Access 10 (2022) 46670–46677, https://doi.org/10.1109/ACCESS.2022.3171326.

[23] L. Gautam, A.J. Amalanathan, R. Sarathi, U.M. Rao, I. Fofana, Effect of magnetic field on partial discharge initiated by metallic particle in thermally aged natural esters under AC and harmonic voltages, IEEE Access 10 (2022) 101198–101206, https://doi.org/10.1109/ACCESS.2022.3208353.

[24] L. Vékás, D. Bica, M.V. Avdeev, Magnetic nanoparticles and concentrated magnetic nanofluids: synthesis, properties and some applications, China Particuol. 5 (2007) 43–49, https://doi.org/10.1016/J.CPART.2007.01.015.

[25] K. Paulovičová, J. Tóthová, M. Rajňák, M. Timko, P. Kopčanský, V. Lisý, Nanofluid based on new generation transformer oil: synthesis and flow properties, Acta Phys. Pol., A 137 (2020) 908–910, https://doi.org/10.12693/APHYSPOLA.137.908.

[26] Z. Rozynek, A. Józefczak, K.D. Knudsen, A. Skumiel, T. Hornowski, J.O. Fossum, M. Timko, P. Kopčanský, M. Koneracká, Structuring from nanoparticles in oil-based ferrofluids, Eur. Phys. J. E (34) (2011) 1–8, https://doi.org/10.1140/EPJE/I2011-11028-5, 2011 343.

[27] N. Pattanadech, M. Muhr, Comments on PDIV testing procedure according to IEC 61294, 2017, IEEE 19th Int. Conf. Dielectr. Liq. ICDL (2017. 2017-January (2017) 1–4, https://doi.org/10.1109/ICDL.2017.8124658.

[28] A.M. Ahmed, A.R. Zakinyan, W.S. Abdul Wahab, Effect of magnetic field on electroconvection in a thin layer of magnetic nanofluid, Chem. Phys. Lett. 817 (2023) 140413, https://doi.org/10.1016/J.CPLETT.2023.140413.

[29] A. Nagornyi, V.I. Petrenko, M. Rajnak, I.V. Gapon, M.V. Avdeev, B. Dolnik, L.A. Bulavin, P. Kopcansky, M. Timko, Particle assembling induced by non-homogeneous magnetic field at transformer oil-based ferrofluid/silicon crystal interface by neutron reflectometry, Appl. Surf. Sci. 473 (2019) 912–917, https://doi.org/10.1016/J.APSUSC.2018.12.197.

[30] S. Nijdam, J. Teunissen, U. Ebert, The physics of streamer discharge phenomena, Plasma Sources Sci. Technol. 29 (2020) 103001, https://doi.org/10.1088/1361-6595/ABAA05.

[31] R. Bartnikas, ASTM International, Electrical Insulating Liquids, ASTM, 1994.

[32] W.G. J, 1980- Hwang, Elucidating the Mechanisms behind Pre-breakdown Phenomena in Transformer Oil Systems, 2010. https://dspace.mit.edu/handle/1721.1/60145. (Accessed 18 September 2023).

[33] M. Huang, L. Zhang, L. Chen, Y. Sheng, M. Niu, Y. Lv, B. Qi, Effects of electron migration and adsorption on the suppression of negative corona discharge in nanoparticle transformer oil: experiments and simulations, J. Phys. D Appl. Phys. 56 (2023) 475203, https://doi.org/10.1088/1361-6463/ACF22B.

[34] J.G. Hwang, M. Zahn, F.M. O'Sullivan, L.A.A. Pettersson, O. Hjortstam, R. Liu, Effects of nanoparticle charging on streamer development in transformer oil-based nanofluids, J. Appl. Phys. 107 (2010), https://doi.org/10.1063/1.3267474/287254.

[35] E.G. Atiya, D.E.A. Mansour, M.A. Izzularab, Partial discharge development in oil-based nanofluids: inception, propagation and time transition, IEEE Access 8 (2020) 181028–181035, https://doi.org/10.1109/ACCESS.2020.3027905.

[36] C. Rablau, P. Vaishnava, C. Sudakar, R. Tackett, G. Lawes, R. Naik, Magnetic-field-induced optical anisotropy in ferrofluids: a time-dependent light-scattering investigation, Phys. Rev. E - Stat. Nonlinear Soft Matter Phys. 78 (2008) 051502, https://doi.org/10.1103/PHYSREVE.78.051502/FIGURES/8/MEDIUM.